Collisional Attenuation of Focused CH_3Cl Molecular Beams in a Hexapole Filter

David A. Blunt,† Sean A. Harris,‡ Wan-ping Hu, and Peter W. Harland*

Chemistry Department, University of Canterbury, Christchurch, New Zealand

Received: September 30, 1997; In Final Form: December 5, 1997

The attenuation of hexapole-focused CH_3Cl molecular beams has been studied as a function of inert gas and nitrogen gas pressure in a hexapole-collision cell. Cross sections have been determined as a function of relative velocity, using seeded beams, and as a function of specific $|JKM\rangle$ states through variation of the electric field strength in the hexapole. Beam attenuation is attributed to rotationally inelastic collisions in which a beam molecule following a focusing upper Stark state ($KM < 0$) trajectory through the hexapole field is converted by a ΔM or ΔJ, ΔM transition into a nonfocusing rotational state ($KM = 0$ or $KM > 0$), which then follows a modified, nonfocusing trajectory and is lost from the beam. Experimental cross sections are in the range from 200 to 670 Å^2, consistent with collisions controlled by a long-range interaction (8 to 15 Å) involving the transfer of a few J mol^{-1} of energy. Collision cross sections estimated using a van der Waals interaction potential with dispersion and dipole−induced dipole terms suggest that cross sections of these magnitudes most probably correspond to collisions in which only the M quantum number changes.

1. Introduction

The transmission efficiency of a hexapole electrostatic filter decreases rapidly with a reduction in vacuum quality; the beam intensity is reduced, and the orientation distribution of the transmitted beam following an adiabatic transition into a weak homogeneous electric field is degraded. The requirement for vacuum quality imposes limitations on the usable range of physical dimensions (rod radius, inscribed radius, and length) for the hexapole assembly. In this study we have attempted to identify the processes responsible for the pressure effects observed and to measure the attenuation cross sections for focused beams of neat and seeded CH_3Cl in a hexapole filter as a function of the electric field strength and the pressure of the scattering gas.

A beam of symmetric top molecules directed into an inhomogeneous hexapole electric field experiences a radial force.[1] Lower Stark states in the beam, for which the rotational quantum number product $KM > 0$, minimize their energy in the field by moving to high field (toward the rods). Such molecules follow rapidly divergent trajectories and are lost from the beam. Upper Stark states, for which $KM < 0$, minimize their energy by moving toward low field and follow trajectories that result in focusing to the axis of the filter, where the field strength is zero. Molecules for which $KM = 0$ are unaffected by the field and assume divergent trajectories defined by the supersonic beam profile and the defining skimmers. The $KM = 0$ component falls off as the reciprocal of the square of the distance from the nozzle and is very much smaller than the focused $KM < 0$ component. The physical size and voltages applied to the rods of the hexapole and the physical properties of the beam gas determine the transmission characteristics for individual $|JKM\rangle$ quantum states transmitted through the filter. For example, in the case of a neat CH_3Cl beam the filter used in this study preferentially focuses the $|111\rangle$ state of CH_3Cl at ±2.4 kV and the $|212\rangle$ state at ±3.7 kV. The focusing voltages for these states in a 5% CH_3Cl in Xe-seeded beam are ±1.2 and ±1.8 kV, respectively.

State-resolved rotationally inelastic scattering of molecules was first studied by Toennies in the early 1960s.[2−4] A velocity-selected effusive beam of TlF was rotationally state selected with an electrostatic quadrupole field. The quadrupole field focused a particular TlF rotational state $|JM\rangle$ into a gas-filled scattering chamber, and a second quadrupole selector placed 1° off-axis was used to analyze the state distribution of the scattered TlF. The cross sections measured for the $|20\rangle \rightarrow |30\rangle$ transition ($\Delta J = 1$) ranged from 2 Å^2 for collisions with He up to 375 Å^2 for collisions with NH_3. The total cross section for loss of the $|20\rangle$ state through all channels (inelastic and elastic) was 152 Å^2 for He collisions up to 2140 Å^2 for NH_3. For collisions involving inert gas atoms the dominant term in the interaction potential was the quadrupole induction potential, but for the symmetric top NH_3 the dipole−dipole interaction term was dominant and the large cross sections were rationalized by the possibility of dipole locking of the TlF and NH_3 molecules. TlF, which exhibits a very high dipole moment (4.23 D) and a large polarizability volume (6.7 Å^3), was used in these experiments because of its desirable focusing properties in the quadrupole field. Because of the large dipole moment and small separation of adjacent J rotational levels in TlF, the energy for ΔJ transitions is available through the quadrupole induction and dipole−dipole terms in the interaction potential at long range, giving large cross sections.

More recently, the same group measured inelastic cross sections for CsF in supersonic Xe-seeded beams.[5,6] Again the CsF was chosen for its large dipole moment and focusing behavior in the quadrupole fields used. The scattering chamber of the earlier experiments was replaced with a crossed beam of the scattering species in order to reduce the averaging effect of the broad velocity distribution of the scattering gas on the cross sections. The gases chosen for the inelastic scattering experiments with the CsF beam included the inert gases, small

* To whom correspondence should be addressed: FAX +64 3 364 2110; p.harland@chem.canterbury.ac.nz.

† Current address: Physical and Theoretical Chemical Laboratory, Oxford University, Oxford, England.

‡ Current address: Chemistry Department, Rice University, Houston, TX.

S1089-5639(97)03166-6 CCC: $15.00
Published on Web 02/05/1998

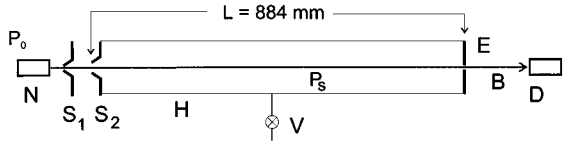

Figure 1. Diagram of molecular beam−hexapole gas cell machine: N = piezoelectric pulsed nozzle, CH_3Cl and seeded beams stagnation pressure P_0 = 2000 Torr; S_1 = 1.0 mm diameter skimmer; S_2 = 1.5 mm diameter skimmer and entrance aperture to hexapole chamber; H = hexapole chamber, total length 884 mm, scattering gas pressure P_s; V = fine metering valve; E = hexapole chamber exit aperture 1.00 mm diameter; B = CH_3Cl molecular beam or 5% CH_3Cl in inert gas seeded beam; D = ion source and quadrupole mass filter molecular beam detector.

molecules such as N_2, CO_2, CH_4, and SF_6, and symmetric top alkyl halides such as CH_3Cl, CH_3Br, CF_3H, CF_3Cl, and CF_3Br. Cross sections for $\{\Delta M = 0, 1; \Delta J = 1, 2\}$ transitions of CsF are reported. They range in magnitude from 0.5 Å^2 for the $|30\rangle \rightarrow |10\rangle$ transition with Kr gas, up to 620 Å^2 for the $|20\rangle \rightarrow |30\rangle$ transition with CF_3H.

2. Experimental Method

An illustration of the molecular beam machine used in this study is shown in Figure 1. Pulsed molecular beams were generated using a piezoelectric nozzle with an open time of 0.1 ms and a repetition rate of 100 Hz from a stagnation pressure of 2000 Torr of pure CH_3Cl or mixtures of 5% CH_3Cl seeded in an inert gas buffer. The beam passed through a 1.0 mm diameter thin-walled skimmer into a buffer chamber and then through a 1.5 mm diameter skimmer into an 884 mm long hexapole collision cell terminated by an exit aperture with an adjustable iris. The hexapole filter was made from six equally spaced 10 mm diameter precision ground stainless steel rods 833 mm in length mounted in glass ceramic (Macor) yokes to give an inscribed radius, r_0, of 5.88 mm. The rods were alternately charged up to ±7 kV to produce an inhomogeneous hexapole electric field up to 1.2×10^6 V m^{-1}. The molecular beam was detected by an Extrel quadrupole mass filter located at the focal point of the filter. Ions produced by the electron impact ionization of gas pulses were gated at the detector, and a second gate of equal width was set to intercept ions produced from the electron impact ionization of the background gas in the chamber prior to the arrival of the gas pulse. The molecular beam was attenuated by admitting a scattering gas into the collision cell through a Leybold Heraeus variable leak valve fitted with a stepping motor and computer controlled. Measurements were taken over a hexapole voltage range from 0 to ±7 kV in 200 V increments for a series of quencher gas pressures over the range from 5×10^{-7} to 5×10^{-5} Torr. Pressures were measured using a model 690 high-accuracy absolute MKS Baratron capacitance manometer with a 0.1 Torr head.

The shape of the defocusing cross section versus hexapole voltage curves was reproducible within a few percent, although the absolute values of the cross sections were ±10%. The maximum calculated error arising from the specifications of the instruments employed in the experiment is around 5%. The lower reproducibility of the absolute cross sections results from the long times, typically 3 h, required to measure the focusing curves for five to eight scattering gas pressures.

In any scattering experiment there will be a certain minimum angular resolution inherent in the apparatus because of the finite size of all beam-collimating apertures. Any scattered beam molecules that are deflected through an angle smaller than the acceptance angle defined by the detector aperture will therefore still be detected, and the measured cross section $\sigma_{\text{eff}}(\bar{g})$ will be the incomplete integral cross section.[7] To extract the complete integral cross section $\sigma(\bar{g})$, a correction must be made for the angular resolution. With the exception of beam molecules suffering a collision very close to the exit aperture, when the mass spectrometer entrance aperture determines resolution, the angular resolution for the convergent upper Stark state beam was deduced by averaging the exit aperture acceptance angle as seen from all points within the length and inscribed radius of the hexapole. This geometrically averaged angular resolution was 24′ for a 1.0 mm exit aperture, although the effective angular resolution is higher because of the focusing−defocusing effect of the hexapole electric field. That is, any rotationally inelastic collision of a focusing upper Stark state beam molecule will produce a rotational state that will not be favorably focused by the hexapole field and the scattered product will be effectively scattered through an angle greater than the initial scattering angle, proportional to the change in ρ ($=KM/J(J+1)$) for the beam molecule in the collision. This further reduces the likelihood of a beam molecule being successfully transmitted through the hexapole exit aperture. Under these conditions the angular resolution correction will be small and it will be rotational state dependent. For a focused beam molecule that suffers a collision accompanied by a small change in ρ there is a greater probability that the scattered beam molecule will still be detected than if the molecule undergoes a transition that brings about a large change in ρ. Hence the cross sections that are measured here will be incomplete cross sections (although the difference from the complete integral cross sections is expected to be small).

The cross section, σ, for the attenuation of the CH_3Cl molecular beam by collisions with scattering gas, s, in the hexapole collision cell was calculated using Beer's law[7]

$$\sigma_{\text{eff}}(\bar{g}) = (n_s L)_{\text{eff}}^{-1} \ln\frac{I}{I_0} \tag{1}$$

where $(n_s L)_{\text{eff}}$ is the product of the path length L and the density n_s averaged over the entire path length. The leakage of the scattering gas through the skimmer and exit aperture will effectively increase the scattering path length. However, the leakage is effusive and falls off rapidly with distance from the aperture; with the exception of helium, the increase in path length due to this end effect will be negligible. The cross section $\sigma_{\text{eff}}(\bar{g})$ is the experimentally measured cross section averaged over the relative velocity distribution $f_r(g)$, where $g = |\mathbf{v}_b - \mathbf{v}_s|$. $\mathbf{v}_b$ is the velocity of the beam with a distribution $f_b(\mathbf{v}_b)$ and $\mathbf{v}_s$ is the velocity of the scattering gas with a distribution $f_s(\mathbf{v}_s)$. The reference velocity for the cross sections was taken here as the average relative velocity, $\bar{g}$

$$\bar{g} = (v_b^2 + v_s^2)^{1/2} \tag{2}$$

where v_s is taken as the most probable velocity for the scattering gas,

$$v_s = \left(\frac{2KT}{m_s}\right)^{1/2} \tag{3}$$

and v_b is the flow velocity measured directly by time-of-flight. I is the measured beam intensity, and I_0 is the beam intensity in the absence of any scattering gas. A plot of ln I versus P is shown in Figure 2 for the attenuation of a neat beam of CH_3Cl by Ar for a hexapole voltage of ±5 kV.

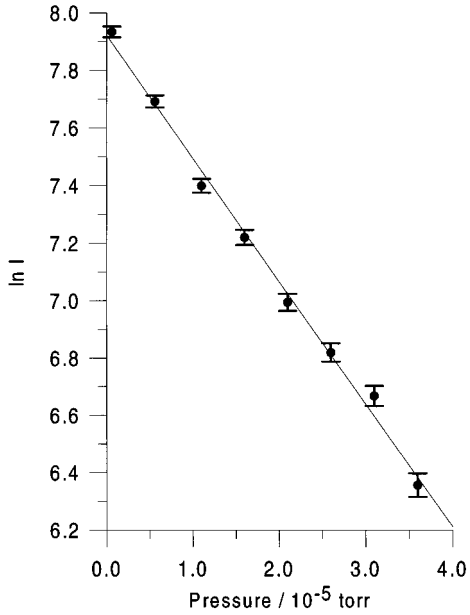

Figure 2. CH_3Cl beam attenuation plot for Ar as scattering gas at a hexapole voltage of ±5 kV.

The beam signal, *I*, corresponding to the transmission of the attenuated upper Stark state (focused) component of the beam for collision cell pressure *P* and a given hexapole voltage, is determined from the difference between the signal recorded with the hexapole on, $I_{on,P}$, and the signal for zero hexapole voltage, $I_{off,P}$. This difference, and the cross section calculated from eq 1, corresponds to the attenuation of upper Stark states by elastic and inelastic scattering corrected for the attenuation of the *MK* = 0 component of the beam. Cross sections calculated from the attenuation of the beam with the hexapole at ground potential corresponded to the elastic and inelastic scattering (changes in ΔJ only since *M* is not defined in the absence of an electric field) of the nonfocused component of the beam. Attenuation cross sections for beams with the hexapole grounded, when the *M* quantum number is not defined, varied from 90 Å^2 for collisions with Ne up to a maximum of about 200 Å^2 for collisions with Xe. These cross sections were dependent on the diameter of the exit aperture, decreasing with increasing diameter as the geometrically averaged angular resolution decreased. This suggests that the beam attenuation in the absence of the field is dominated by small-angle scattering through elastic collisions. The cross sections measured for the attenuation of the focused beams of CH_3Cl were independent of the exit aperture diameter below 6.0 mm, strongly suggesting that the process dominating the attenuation of the focusing beam involves large-angle scattering, as would be expected following an inelastic collision with a concomitant change in the molecular trajectory in the inhomogeneous electric field. All cross sections reported here were measured with a 1.0-mm exit aperture.

Since the determination of the cross section with the hexapole energized requires upper Stark states to be focused by the hexapole, the cross sections will only be defined for hexapole voltages greater than the hexapole voltage threshold for the focusing of upper Stark states given by[8]

$$U_0 = \frac{\pi^2 r_0^{\,3}}{6L^2}\frac{m_b v_b^{\,2}}{\mu_b} \qquad (4)$$

where r_0 and *L* are the inscribed radius and length of the hexapole, respectively, and m_b, v_b, and μ_b are the mass, velocity, and electric dipole moment of the beam molecule, CH_3Cl, in the hexapole field. Below the threshold the difference between hexapole-on and hexapole-off signals results from noise only.

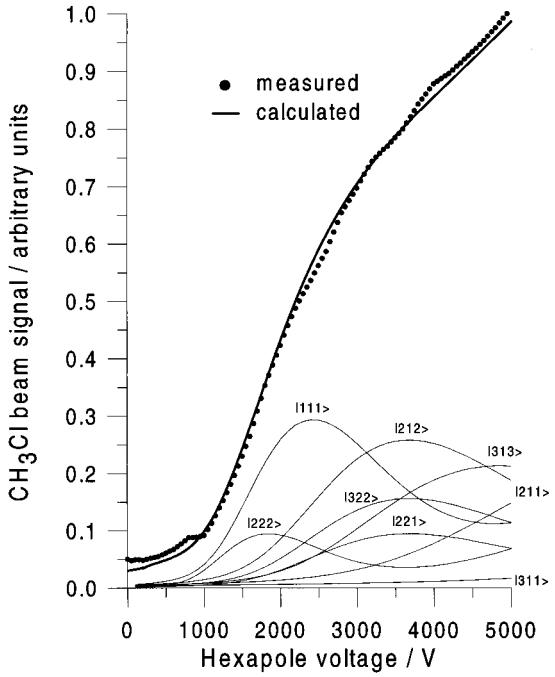

Figure 3. Calculated (—) hexapole transmission curve for a neat beam of CH_3Cl at 15 K compared to an experimental (●) curve. Only rotational states with *J* and $K \leq 5$ were included in the calculation. Calculated transmission curves for the most significant $|JKM\rangle$ contributing states ($KM < 0$) to the overall transmission curve are also included.

3. Results

An experimental hexapole transmission curve for a neat beam of CH_3Cl is shown in Figure 3. A good fit between the measured and calculated[1] transmission curves was obtained for a CH_3Cl rotational temperature of 10 K $\leq T_J = T_K \leq$ 15 K with $K \leq 3$ and $J \leq 5$. This is consistent with the large difference between the rotational constants about the symmetry and perpendicular axes of CH_3Cl which favors the population of states with low values of *K*. The transmission curves calculated for the individual $|JKM\rangle$ quantum states show broadening due to the velocity distribution characteristic of the beam and to the range of trajectories defined by the skimmers and hexapole entrance aperture. The major contributions to the transmission curves under the experimental conditions are from the $|111\rangle$, $|212\rangle$, $|313\rangle$, and $|211\rangle$ states (at 7 kV), and these transmission curves are shown in Figure 3. The effect of pressure on the transmission curve for a neat beam of CH_3Cl is shown in Figure 4. The attenuation of the curve shows structure that is not evident in the absence of inelastic collisions. The minima in the attenuated curve corresponding to enhanced attenuation result from a more efficient scattering of molecules transmitted at those hexapole voltages, and they match the peaks in the transmission curves for the most highly populated $|JKM\rangle$ states.

Figure 5 shows the cross sections for attenuation of seeded CH_3Cl beams by argon as a function of the hexapole voltage, and Figure 6 shows curves for collisions of a 5% CH_3Cl seeded in Kr beam with the inert gases and nitrogen. The calculated peak hexapole voltage corresponding to a given $|JKM\rangle$ state is dependent on the beam composition; for example, the $|111\rangle$ state peaks at ±2.4 kV for a neat beam, ±2.3 kV for a 5% CH_3Cl in Ar beam, ±2.0 kV for a 5% CH_3Cl in Kr beam, and ±1.2 kV for a 5% CH_3Cl in Xe beam. The cross section profiles for all

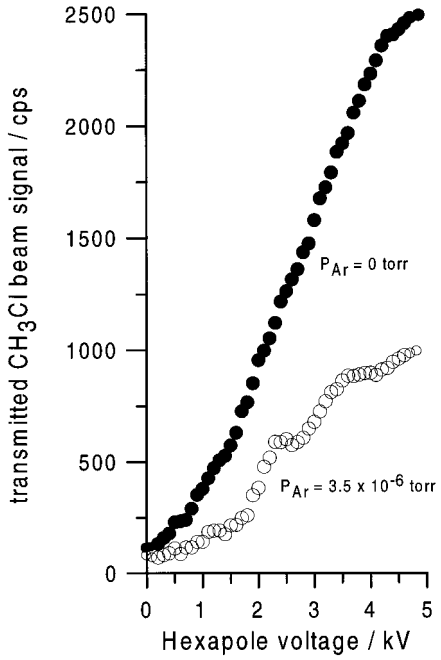

Figure 4. Experimental CH_3Cl hexapole transmission curves in the absence and presence of Ar scattering gas in the hexapole collision cell.

beam-scattering gas combinations exhibit three reasonably well-defined maxima (or shoulders) corresponding to the calculated peak focus for the $|111\rangle$, $|211\rangle$, and $|212\rangle$ states, as shown in the figures. The cross sections are large, indicative of a long-range interaction. The quality of the data is not high, and valid conclusions regarding the inelastic process responsible for beam attenuation can be made without attempting to extract further details by curve-fitting methods.

The cross sections for the attenuation of the focused beams increase with decreasing relative velocity, i.e., as the mass of the buffer gas increases, Figure 5**,** and as the mass of the scattering gas increases, Figure 6. In each of these figures, the first peak in the cross section profile exhibits a maximum corresponding with the position for peak focusing of the $|111\rangle$ state. The hexapole voltages corresponding to the calculated peak in the transmission curves for the four dominant $|JKM\rangle$ states over the voltage range accessible in the experiments are marked in the figures.

4. Discussion

Attenuation cross sections fall in the range from 200 Å^2 for collisions of neat CH_3Cl beams on Ne to 670 Å^2 for 5% CH_3Cl in Xe seeded beams on N_2. These cross sections correspond to defocusing interactions for particle separations over the range from 8 to 15 Å. The interaction potential at these separations is dominated by the attractive van der Waals interaction $V(r)$ of the form

$$V(r) = -\frac{C}{r^s} \tag{5}$$

Nonreactive scattering cross sections, $\sigma(\bar{g})$, are expected to show a velocity dependence[9−11] such that

$$\sigma(\bar{g}) \propto \bar{g}^{-2/(s-1)} \tag{6}$$

where $\bar{g}$ is the average relative velocity of the collision partners. For a van der Waals attractive force $s = 6$. From eq 6 the velocity dependence of the attenuation cross sections should

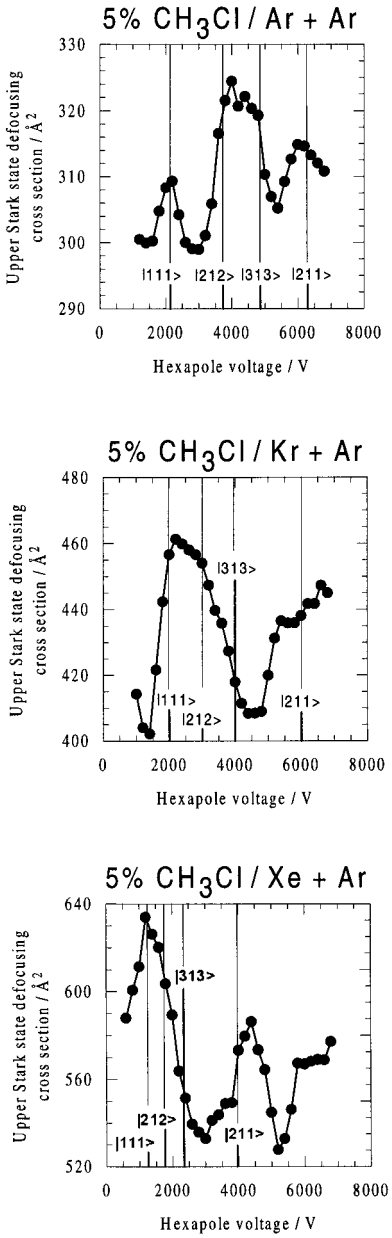

Figure 5. Variation of cross sections for the attenuation or defocusing of CH_3Cl seeded beams on Ar scattering gas as a function of hexapole voltage. Hexapole voltages corresponding to the peak transmissions of the most significant $|JKM\rangle$ states present in the beam are shown for each seeded beam.

exhibit a $\bar{g}^{-0.4}$ dependence. Figure 7a is a plot of the cross sections corresponding to the attenuation of the $|111\rangle$ state of CH_3Cl for collisions of neat and seeded beams with the inert gases and nitrogen plotted against $\bar{g}^{-0.4}$, which was calculated from eqs 2 and 3. There is a good correlation between $\sigma(\bar{g})$ and $\bar{g}^{-0.4}$ over a wide range of velocity and cross sections, lending support for energy transfer under the influence of an interaction potential of the form

$$V(r) = -\frac{C}{r^6} \tag{7}$$

where C accounts for the dipole and polarization interactions. For inelastic collisions between polarizable neutral species in which only one of the them exhibits a permanent dipole moment only the London dispersion and dipole−induced dipole terms need to be considered.

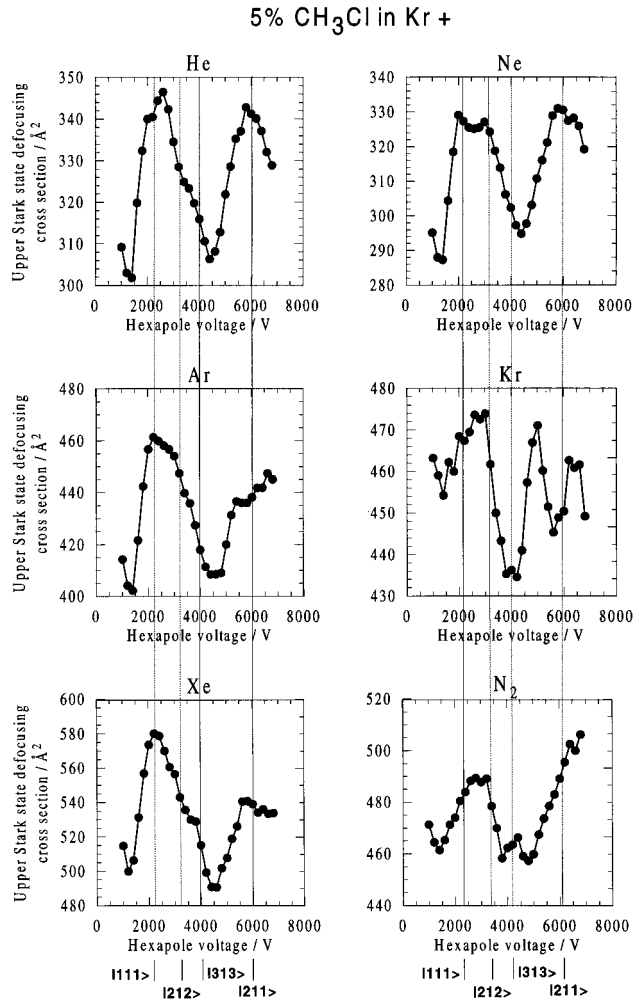

Figure 6. Variation of cross sections for the attenuation or defocusing of 5% CH_3Cl in Kr seeded beams on the inert gases and nitrogen as a function of hexapole voltage. Hexapole voltages corresponding to the peak transmissions of the most significant $|JKM\rangle$ states present in the 5% CH_3Cl in Kr beam are shown.

$$C = C_{\text{disp}} + C_{\text{dip-ind dip}} \tag{8}$$

where

$$C_{\text{disp}} = \frac{3}{2}\alpha_b\alpha_s\frac{E_{0,b}E_{0,s}}{E_{0,b} + E_{0,s}} \tag{9}$$

and

$$C_{\text{dip-ind dip}} = \frac{\mu_b{}^2\alpha_s}{4\pi\epsilon_0} \tag{10}$$

α and E_0 are polarizability volumes and ionization potentials, respectively, and μ_b is the dipole moment of CH_3Cl.[12]

To facilitate a rotational transition of energy ΔE_R, the maximum separation for the particles is given by

$$r_{\text{max}} = \left|\left(\frac{C}{\Delta E_R}\right)^{1/6}\right| \tag{11}$$

and the maximum cross section by $\pi r_{\text{max}}{}^2$ or

$$\sigma_{\text{max}} = \pi\left(\frac{C}{\Delta E_R}\right)^{1/3} \tag{12}$$

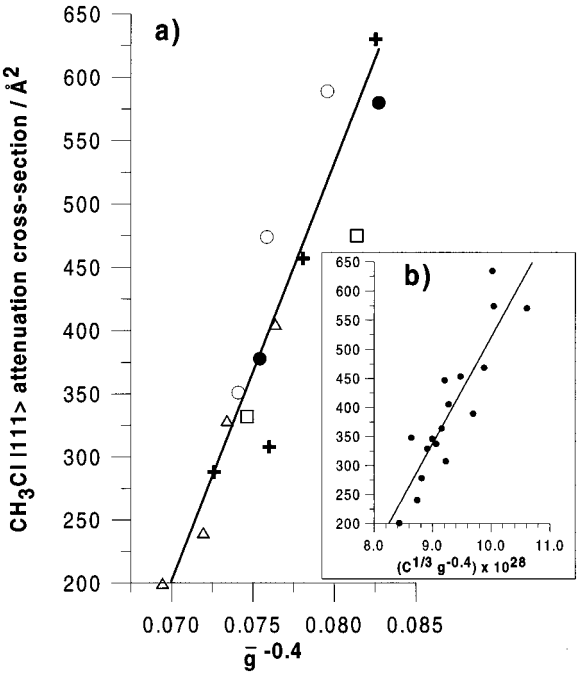

Figure 7. (a) Plot of the attenuation or defocusing cross sections for the $|111\rangle$ state of CH_3Cl for collisions of neat and seeded beams on inert gas and nitrogen-scattering gases plotted against $\bar{g}^{-0.4}$, where $\bar{g}$ is the relative collision velocity. Open triangles are neat and seeded beams of CH_3Cl with Ne as the scattering gas, open circles for N_2, crosses for Ar, open squares for Kr, and closed circles for Xe. (b) Cross sections in plot a plotted against $C^{1/3}\bar{g}^{-0.4}$.

An r^{-6} interaction potential requires that the cross section for a transition of energy ΔE_R should exhibit a $C^{1/3}$ dependence. Incorporating the velocity dependence described in eq 6, there should be a linear relationship between the attenuation cross section for a specific transition and the product $C^{1/3}\bar{g}^{-0.4}$. The cross section data plotted against $\bar{g}^{-0.4}$ in Figure 7a is replotted against $C^{1/3}\bar{g}^{-0.4}$ in Figure 7b, giving an acceptable straight line fit.

The spectroscopic selection rules for rotational-state transitions of symmetric top molecules[13] are $\Delta J = 0, \pm 1$; $\Delta K = 0$; and $\Delta M = 0, \pm 1$. For the attenuation of focused upper Stark states in the hexapole electric field the product JKM must be nonzero and KM must be negative. The only transitions allowed by these selection rules leading to the defocusing of upper Stark states are

$$\Delta J = 0;\ \Delta M = \pm 1, \text{ where } J > 0 \text{ and } |M| \le J$$

and

$$\Delta J = \pm 1;\ \Delta M = 0, \pm 1, \text{ where } J > 0 \text{ and } |M| \le J$$

The Dirac notation used to describe rotational quantum states by convention omits the negative sign required for an upper Stark state. That is, $|JKM\rangle$ is used instead of $|J\text{-}KM\rangle$ or $|JK\text{-}M\rangle$.

Oka et al.[14,15] investigated the selection rules that apply during rotationally inelastic collisions in NH_3, H_2CO, and CH_3F using inverse Lamb dips in infrared laser Stark spectroscopy. Collision-induced transitions with $\Delta M > 1$ were identified in the H_2CO system, although cascading could not be totally eliminated. Analysis of very large signals for $J = K$ levels of CH_3F indicated that the rate of $\Delta M = \pm 1$ reorientation collisions relative to all inelastic collisions was on the order of 70%. It

was also noted that transitions for which $\Delta M > 1$ would increase this proportion.

The $|111\rangle$ state of CH_3Cl can be attenuated by allowed transitions to the $|110\rangle$, $|210\rangle$, $|211\rangle$, and $|212\rangle$ states. The first two states are unaffected by the hexapole electric field and will not be focused back to the hexapole exit aperture. The second pair of states are upper Stark states, but as their cos θ values are 1/6 and 1/3, respectively, compared to 1/2 for the $|111\rangle$ state, they will focus at different hexapole voltages and will not be transmitted at the peak hexapole voltage for focusing of the $|111\rangle$ state.

The rotational energy levels $W(JKM)$ for a prolate symmetric top in a hexapole field are given by[13]

$$W(JKM) = BJ(J+1) + (A-B)K^2 - \mu\epsilon\frac{KM}{J(J+1)} \quad (13)$$

where A and B are the rotational constants and ϵ is the radial field strength in the hexapole filter. The Stark energies are therefore dependent on the hexapole electric field strength, which varies from a maximum near the hexapole rods to zero at the axis. For a CH_3Cl beam following a trajectory with a displacement $r_0/2$ from the axis, the ΔM transition energy is 0.76 J mol^{-1}. ΔJ and ΔK transition energies are 20.7 and 56.4 J mol^{-1}, respectively.

A theoretical study of M-changing collisions in CH_3X (X = F, Cl, Br, and I) molecules was carried out by Phillips on the basis of these experiments.[16] Phillips calculated attenuation cross sections specifically for our machine using time-dependent perturbation theory and a van der Waals potential for dipole−induced dipole interactions. The calculated "total" relaxation cross section corresponding to an M-changing collision for CH_3Cl−Ar at a hexapole voltage of ±5 kV was ∼60 Å^2 compared with measured cross sections in the range 300 Å^2 for a neat CH_3Cl beam to 550 Å^2 for a 5% CH_3Cl/Xe beam at ±5 kV. While Phillips argues convincingly the involvement of ΔM transitions and a long-range van der Waals potential in the relaxation process, a dispersion term contribution to the potential was not included and this would result in an underestimation of the cross sections. The inclusion of a dispersion term in these calculations will increase the cross section by a factor of 2 or 3. Since the cross sections measured in this work are up to an order of magnitude greater than the calculated values, the participation of a longer range process than required to account for ΔJ transitions appears most likely.

Upper limits to cross sections can be calculated for any transition energy using eqs 8−12. For example, the defocusing transitions from the $|111\rangle$ state of CH_3Cl in collisions with Ar scattering gas are

(i) $|111\rangle \rightarrow |110\rangle$ ($\Delta J = 0$; $\Delta M = \pm 1$)

(ii) $|111\rangle \rightarrow |211\rangle$ ($\Delta J = +1$; $\Delta M = 0$)

(iii) $|111\rangle \rightarrow |210\rangle, |212\rangle$ ($\Delta J = +1$; $\Delta M = \pm 1$)

From eqs 8−10, $C = 1.2275 \times 10^{-77}$ J m^6. Applying eqs 11 and 12: (case i) $r_{max} = 14.6$ Å, $\sigma_{max} = 670$ Å^2; (case ii) 8.4 and 222 Å^2; (case iii) 8.4 Å, 220 Å^2 and 8.5 Å, 226 Å^2. If K-changing transitions were allowed, the higher energy would place an upper limit of 159 Å^2 on the cross section for a $K = 2 \leftarrow K = 1$ transition. These calculated cross sections are upper limits: (i) they do not take into account the influence of collision velocity on the efficiency of energy transfer; (ii) they assume an opacity function of unity; (iii) they are calculated for a hexapole field (ΔM transition energies) corresponding to trajectories with a maximum axial displacement of $r_0/2$. M-changing transitions will be of higher energy for those molecules sampling a higher hexapole field, $r > r_0/2$, giving a lower calculated cross section. The cross sections measured for the attenuation of the $|111\rangle$ state of CH_3Cl depend on the relative collision velocity, as shown in Figure 7. The attenuation cross section varied from 630 Å^2 at the lowest collision velocity (5% CH_3Cl in Xe beam) to 200 Å^2 for the highest collision velocity (neat CH_3Cl beam). The lowest experimental values, corresponding to the highest collision velocity, are higher than the calculated values for a ΔJ, ΔM transition and lower than the cross section calculated for a $\Delta M = 1$ transition. The highest experimental value, corresponding to the lowest collision velocity, is much closer to the value calculated for a $\Delta M = 1$ transition. This also applies to the other scattering gases, and the results are summarized in Table 1, which shows the calculated cross sections corresponding to attenuation of the $|111\rangle$ state of CH_3Cl for collisions with all the inert gases and nitrogen compared with the minimum and maximum values measured.

TABLE 1: Calculated and Measured Cross Sections for Collision-Induced Rotational Transitions from the $|111\rangle$ State of CH_3Cl at the Hexapole Voltage Corresponding to Peak Transmission

scattering gas	$C/10^{-77}$ J m^6	σ(calc)/Å^2 $\Delta J = 1$, $\Delta M = \pm 1$	σ(calc)/Å^2 $\Delta J = 1$, $\Delta M = 0$	σ(calc)/Å^2 $\Delta J = 0$, $\Delta M = \pm 1$	σ(expt)/Å^2 range
Ne	0.372	<149, <153	<150	<450	200−410
Ar	1.227	<220, <226	<222	<670	270−630
Kr	2.028	<260, <269	<263	<793	330−580
Xe	3.128	<301, <311	<304	<916	360−580
N_2	1.511	<236, <244	<239	<719	357−620

To assess the reliability of the cross sections calculated using the van der Waals interaction potential, rotationally inelastic cross sections were calculated for some of the TlF + inert gas collisions reported by Toennies.[2] The bond length used to calculate the moment of inertia for TlF was estimated from the bond lengths for TlCl and TlBr to be 2.4 Å. In all cases, the calculated cross sections are too high; for example, the cross sections calculated for a $\Delta J = 1$ ($J' = 1 \leftarrow J'' = 2$) transition in TlF + He, Ar, and N_2 are 236, 451, and 462 Å^2, respectively, compared with the values of 152, 388, and 343 Å^2 reported by Toennies[2] for $J' \leftarrow J'' = 2$ transitions. So, the calculated cross sections in Table 1 are overestimated upper limits. Taking this into account and considering the large values for the cross sections measured at the lower collision velocities, it seems likely that the mechanism responsible for the collisional attenuation of the upper Stark states in the beam is through M-changing transitions involving energy transfer of <1 J mol^{-1}.

The magnitude of the cross sections measured for the attenuation of the $|211\rangle$ and $|212\rangle$ states are not too different from the $|111\rangle$ state. The cross sections calculated from the van der Waals potential for $J' = 3 \leftarrow J'' = 2$ and $J'' = 2 \rightarrow J' = 1$ transitions are lower than those calculated for a $\Delta J = 1$ transition, thereby increasing the gap between the calculated upper limits and the experimental values for the cross sections. Again these data support an M-changing mechanism for the attenuation of focused upper Stark states through collisions in the hexapole filter.

5. Conclusion

The attenuation of rotational quantum state defined focused beams of CH_3Cl in collisions with the inert gases and nitrogen have been measured. Cross sections plotted as a function of the focusing voltage on the hexapole filter exhibit structure that can be identified with the attenuation of specific $|JKM\rangle$ states

of the CH_3Cl beam. The attenuation cross sections are velocity-dependent and show the behavior characteristic of a nonreactive process under the influence of a long-range van der Waals interaction potential. The magnitudes of the attenuation cross sections corresponding to the hexapole focusing voltage for transmission of the $|111\rangle$ state are higher than might be expected for a pure ΔJ transition or for a ΔJ, ΔM transition. Deductions based on the assumption that the process is well-described by a van der Waals potential with dispersion and dipole−induced dipole terms suggest that the attenuation of the CH_3Cl beams by collision as they pass through the hexapole field most likely correspond to changes in the M quantum number. This mechanism for beam attenuation is supported by the analysis of collision-induced Lamb dips in the laser Stark Lamb dip spectroscopy of NH_3, H_2CO, and CH_3F carried by Oka et al.[14,15] and the theoretical cross sections for M-changing collisions between symmetric top molecules and rare gas atoms calculated by Phillips.[16]

Acknowledgment. We should like to acknowledge the Marsden Fund for support of this project through Contract UOC605, which also provided a graduate fellowship for Wanping Hu, and we would like to express our thanks to Phil Brooks for helpful suggestions and comments.

References and Notes

(1) Brooks, P. R.; Harland, P. W. *Advances in Gas-Phase Ion Chemistry*; Adams, N. G., Babcock, L. M., Eds.; JAI Press: London, 1996; Vol. 2.

(2) Toennies, J. P. *Faraday Discuss. Chem. Soc.* **1962**, *33*, 96.

(3) Toennies, J. P. *Z. Phys.* **1965**, *182*, 257; **1966**, *193*, 76.

(4) Bennewitz, H. G.; Kramer, K. H.; Paul, W.; Toennies, J. P. *Z. Phys.* **1964**, *177*, 84.

(5) Borkenhagen, U.; Malthan, H.; Toennies, J. P. *Chem. Phys. Lett.* **1976**, *41*, 222.

(6) Borkenhagen, U.; Malthan, H.; Toennies, J. P. *J. Chem. Phys.* **1979**, *71*, 1722.

(7) Buck, U. *Atomic and Molecular Beam Methods*; Scoles, G., Ed.; Oxford University Press: Oxford, 1988; Vol. 1.

(8) Chakravorty, K. K.; Parker, D. H.; Bernstein, R. B. *Chem. Phys.* **1982**, *68*, 1.

(9) Landau, L. D.; Lifshitz, E. M. *Quantum Mechanics*; Pergamon Press: New York, 1958.

(10) Massey, H. S. W.; Mohr, C. B. O. *Proc. R. Soc. A* **1934**, *144*, 188.

(11) Massey, H. S. W.; Burhop, E. H. S. *Electronic and Ionic Impact Phenomena*; Oxford University Press: Oxford, 1952.

(12) For example: Atkins, P. W. *Physical Chemistry*, 6th Ed.; Oxford University Press: Oxford, 1994; Chapter 22.

(13) Townes, C. H.; Schawlow, A. L. *Microwave Spectroscopy*; McGraw-Hill Book Co. Inc.: New York, 1955.

(14) Johns, J. M. C.; McKellar, A. R. W.; Oka, T.; Römheld, M. *J. Chem. Phys.* **1975**, *62*, 1488.

(15) Oka, T. *Adv. Atomic Mol. Phys.* **1973**, *9*, 127.

(16) Phillips, L. F. *J. Chem. Soc., Faraday Trans.* **1995**, *91*, 4363.